Waste and Biomass Valorization (2021) 12:3575–3587
https://doi.org/10.1007/s12649-020-01279-9

SHORT COMMUNICATION

One-Pot Biosynthesis of Maghemite (γ-Fe_2O_3) Nanoparticles in Aqueous Extract of *Ficus carica* Fruit and Their Application for Antioxidant and 4-Nitrophenol Reduction

Brajesh Kumar[1,2] · Kumari Smita[1] · Salome Galeas[3] · Victor H. Guerrero[3] · Alexis Debut[1] · Luis Cumbal[1]

Received: 26 June 2020 / Accepted: 12 October 2020 / Published online: 17 October 2020

Abstract

Nowadays, iron oxide based nanomaterials are well known for their multifunctional properties and their applications in various fields. In this article, a simple, one pot and green method for the biosynthesis of single phase maghemite (γ-Fe_2O_3) nanoparticles using an aqueous fruit extract of *Ficus carica* were reported. A detailed spectroscopic and microscopic analysis based on UV–Vis, XRD, FTIR, TGA, DLS, TEM and SAED were used to establish the optical property, morphology, composition, purity, nature and other properties of the synthesized γ-Fe_2O_3 NPs. UV–Vis, FTIR and TGA analysis indicated the involvement of phytochemicals of *Ficus carica* fruits in nanoparticle synthesis and direct functionalization of nanoparticle surfaces. XRD pattern confirmed the purity and nature of well-crystallized γ-Fe_2O_3 NPs. DLS showed the average hydrodynamic size of γ-Fe_2O_3 NPs while, TEM micrographs confirmed the formation of spherical and 4–6 nm sized γ-Fe_2O_3 NPs. In addition, the γ-Fe_2O_3 NPs showed (a) free radical scavenging activity against DPPH and (b) catalytic activity for the reduction of 4-Nitrophenol in the presence of $NaBH_4$. This biosynthetic method provided an advantageous pathway to fabricate bulk quantities of γ-Fe_2O_3 NPs and maybe extend their applications in different biotechnological applications.

✉ Brajesh Kumar
krmbraj@gmail.com; krmbrajnano@gmail.com

[1] Centro de Nanociencia y Nanotecnologia, Universidad de Las Fuerzas Armadas ESPE, Av. Gral. Rumiñahui s/n, P.O. BOX 171-5-231B, Sangolqui, Ecuador

[2] Post Graduate Department of Chemistry, TATA College, Chaibasa, Jharkhand 833202, India

[3] Laboratorio de Nuevos Materiales, Departamento de Materiales, Escuela Politecnica Nacional, Quito, Ecuador

Graphic Abstract

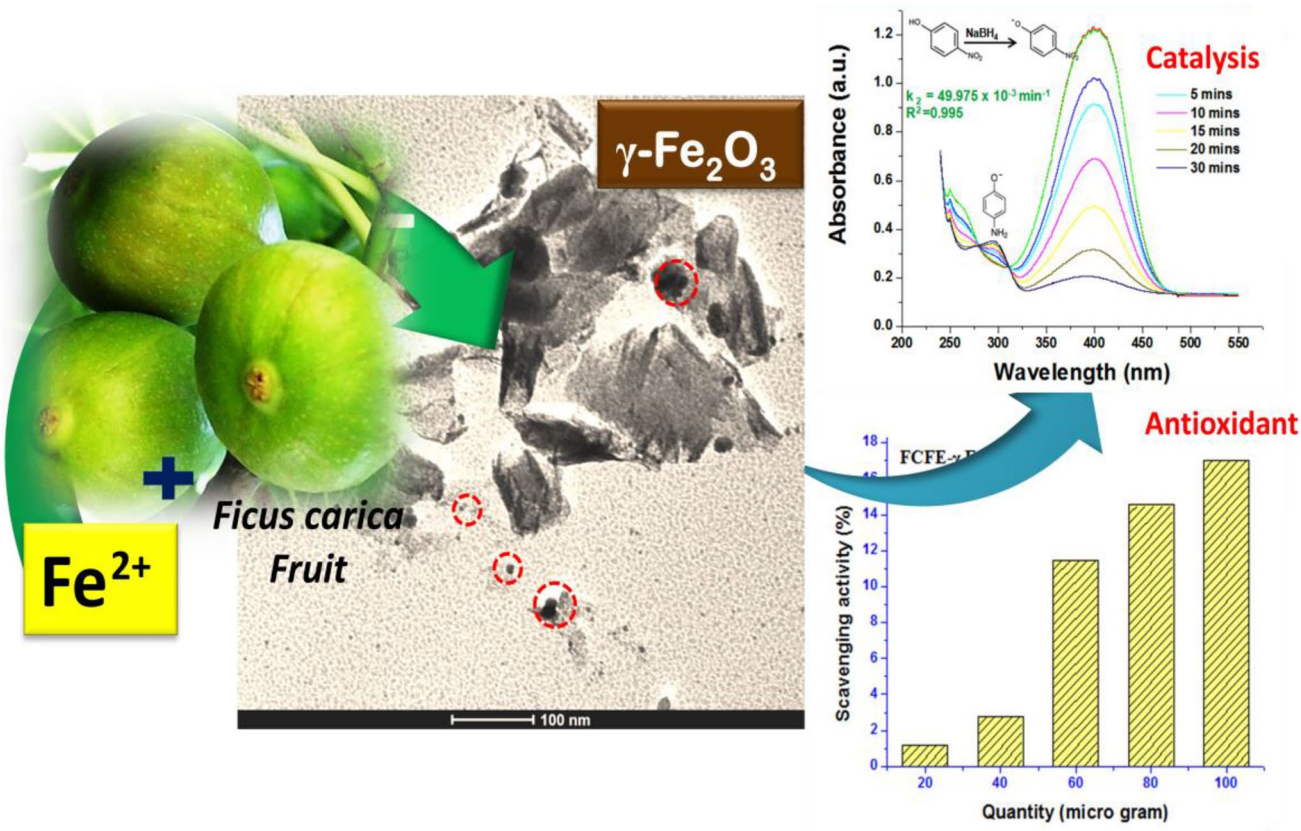

Keywords Green synthesis · *Ficus carica* fruit · γ-Fe_2O_3 nanoparticles · Spectroscopy · Catalyst · Antioxidant

Statement of Novelty

The development of facile and low-cost methods to synthesize ultrasmall (2–20 nm) maghemite nanoparticles with naturally occurring plant materials is an emergent and timely necessity for scientific community worldwide. In this study, single phase γ-Fe_2O_3 NPs was synthesized using fruit extract of *Ficus carica*; confirmed by various spectroscopic and microscopic techniques. It also showed considerable antioxidant and catalytic activity.

Introduction

Iron (Fe) is a 4th abundant metal in the earth's crust representing the essential elements which are absolutely critical to the biological processes [1]. It exists mostly in the form of Fe^0, and oxides of Fe^{2+}/Fe^{3+} as wustite (FeO), magnetite (Fe_3O_4), hematite (α-Fe_2O_3) and maghemite (γ-Fe_2O_3) forms. Since the early 1990s, the ultrafine iron oxide nanoparticles (FeONPs) has been taken special attention by researchers from various fields due to their outstanding multifunctional properties such as small size, high surface area to volume ratio, high magnetism, thermal stability, biocompatibility and low toxicity compared to other nanoparticles [2]. Therefore, FeONPs are frequently assessed for their potential nanotechnology related applications in magnetic fluids, magnetic recording devices, high-frequency switch modes, electromagnetic absorbers [3], catalysis, dye/antibiotic degradation, [4], nano-biomedicines, cosmetics, diagnostics, sensing [5], heavy metal absorption, waste water treatment, material sciences, etc. [6, 7]. Among different iron oxides, γ-Fe_2O_3 is a very common ferrimagnetic mineral on the earth's surface, stable to aqueous conditions, enhanced adsorbing abilities, chemical stability, nontoxicity and exhibit the cubic spinel structure [1]. The use of nanoparticles in different field has escalated 25 fold from 2005 to 2010 [8]. Various chemical and physical synthetic approaches widely used for preparing maghemite nanoparticles (γ-Fe_2O_3NPs) including aerosol/ vapour (pyrolysis), gas deposition, sol–gel, co-precipitation, electrochemical,

microemulsion, flow injection, bulk solution, hydrothermal and solvo-thermal method, etc. [9, 10]. But, only few solutions-based synthetic routes are recommended and scaled up for industrial-scale production due to their low operating cost, biological compatibility and safety issue [11, 12]. However, controlled synthesis of γ-Fe_2O_3 NPs with such specific morphology is still challenging. Generally, FeONPs are chemically robust and can be oxidized easily with air. Therefore, it is necessary to maintain their stability by promising protection tactics and to coat their surface with biomolecules, organic molecules, polymers, or inorganic layer [13].

In recent years, the one-pot biosynthesis of γ-Fe_2O_3 NPs using extracts of natural products as reducing and capping agent has been considered as a simple, cost effective and environmentally friendly alternative to chemical and physical methods of nanoparticle production [14, 15]. Phytochemicals in plant extract simply convert $Fe^{2+/3+}$ to Fe^0/FeO NPs due to difference between the standard reduction potential of phytochemicals (0.534 V) and metallic iron (− 0.44 V), and therefore the reduction process is spontaneous [15]. While there are many studies concerning on the biosynthesis of γ-Fe_2O_3 NPs using various plant materials such as (a) leaf extracts of *Castanea sativa* [14], Omani mango [16], Tea [17] and Oolong tea [18], *Tridax* [19], *Peltophorum pterocarpum* [20], Iranian Mango [21], *Rhamnella gilgitica* [22], *Sageretia thea* [23]; (b) fruit extracts of *Hyphaene thebaica* [24] *Ficus carica* [25], (c) dried bark of *Cinnamomun verum* and (d) dried pods of *Vanilla planifolia* [26] has been already reported. Singh et al. reported superparamagnetic starch functioned γ-Fe_2O_3 NPs for the removal of Chromium [27], whereas Duman et al. used blooming microalgae mediated synthesis γ-Fe_2O_3 NPs for biofuel production [28]. Therefore, the development of facile and low-cost methods to synthesize ultrasmall (2–20 nm) γ-Fe_2O_3 NPs with naturally occurring plant materials is an emergent and timely necessity for scientific community worldwide.

Ficus carica (*F. carica*), is native to South-West Asian countries, and the Mediterranean region [29]. Fruits are edible, axillary on leafy branchlets, pear shaped, often get cracked on ripening. The interior portion of fruit is a white, inner ring containing a seed mass bound with sweet jelly-flesh. Seeds are numerous in number and vary in size [30]. Fruit contains flavonoids, coumarins, and major phytochemicals of anthocyanin class, namely, glycosides of cyanidin, pelargonidin and peonidin [31].

Nitroaromatic compounds are the most common organic pollutant that exists in industrial and agricultural wastewaters. 4-nitrophenol (4-NP) and 2-nitrophenol (2-NP) are examples of toxic substance that are stable in aqueous media and have been classified as a priority toxic pollutant by the U.S. Environmental Protection Agency (EPA) [32]. Nitrophenolic wastes are carcinogenic, and cause hepatotoxicity and mutagenesis in living organisms so they need to be removed from aqueous media. The removal of nitrophenol from aqueous media or catalytic transformation into valuable compounds such as amino phenols have been widely used with $NaBH_4$ through catalytic reduction reactions by the colloidal metallic nanoparticles like gold, silver, iron, cobalt, nickel and copper [33, 34].

In this report, we have developed a facile, low-cost and ecofriendly method for the one-pot biosynthesis of single phase γ-Fe_2O_3 NPs using unripened fruit extracts of *F. carica* as a natural resource.The rich phytochemicals of the plant extracts is responsible for reducing and stabilizing the nanoparticles. The obtained γ-Fe_2O_3 NPs have been examined by various analytical tools including U.V.-Vis spectroscopy, XRD, FTIR, TGA, TEM-SAED and DLS. In addition to this, the synthesized γ-Fe_2O_3 NPs were used as an antioxidant for scavenging free radical against DPPH and catalyst for the reduction of 4-NP to 4-AP.

Experimental

Materials

All chemicals were reagent grade and used without any purification. $FeSO_4{\cdot}7H_2O$ (99.0%) and 4-Nitrophenol (> 99.5%, 4-NP) were purchased from Spectrum, USA. 1, 1-diphenyl-2 picrylhydrazyl (DPPH·, > 99.5%) and Sodium borohydride ($NaBH_4$, > 99.5%) were purchased from Sigma-Aldrich, USA. Milli-Q water was used in all experiments. All glassware was washed with acid/base solution followed by Milli Q water and finally dried in a hot air oven.

Preparation of Aqueous Extract of *Ficus carica* Fruit (FCF)

In this experiment unripened *F. carica* fruit was collected from the garden of Playa Chica 1 near Universidad de las Fuerzas Armadas ESPE, Sangolquí, Ecuador and washed with Milli Q water to remove dust particles. Aqueous extract of *F. carica* fruit (FCFE) was prepared as per our earlier report [35]. About 20 g of thoroughly washed unripe *F. carica* fruit was chopped finely (0.5–0.8 cm) and heated in 100 mL of Milli-Q water for 60 min at 65–70 °C. The light yellow extract was filtered through a Whatmann paper No. 2 to eliminate particulate substance. The clear filtrate was used for the synthesis of nanoparticles and stored at 4 °C for subsequent experiments.

Biosynthesis of γ-Fe_2O_3 NPs

For the biosynthesis γ-Fe_2O_3 NPs via co-precipitation, 25 mL of $FeSO_4{\cdot}7H_2O$ (4 mM, 27.8 mg) was mixed with 10 mL of FCE extract (68.2279 µg GAE, Gallic acid

equivalents) and pH is adjusted to 9–10 using 0.1 M KOH solution. After that, as-prepared greenish-blue colour reaction mixture was kept under vigorous magnetic stirring for 2 h at 78–80 °C. The visual colour change from greenish-blue to brownish-black indicated that the γ-Fe_2O_3 NPs were formed (Fig. 1a). The resulting γ-Fe_2O_3 NPs were centrifuged at 8000 rpm for 2 × 15 min and washed several times with 1:1 mixtures of distilled water, and absolute methanol. The Purified γ-Fe_2O_3 NPs powder was dried at 90 °C for 12 h and stored in an airtight bottle for further analytical characterization by UV–Vis, XRD, FTIR, TGA, TEM, and DLS.

Morphology and Physicochemical Characterization of γ-Fe_2O_3 NPs

The optical properties of samples containing FCF extract and γ-Fe_2O_3 NPs were recorded by using UV–Visible spectrophotometer, SPECORD® S600 from Analytik Jena, Germany. Crystal structure identification of nanoparticle was achieved by X-ray diffraction (XRD) analyses with a PANalytical brand θ–2θ configuration (generator-detector) X-ray tube, copper λ = 1.54 Å and EMPYREAN diffractometer. The FTIR- attenuated total reflection (ATR) spectra were collected in the transmission mode (4000–400 cm^{-1}) using a Spectrum 100 IR spectrometer (Perkin Elmer, USA) to determine the possible involvement of functional groups for the synthesis of nanoparticles. The thermogravimetric analysis (TGA) was carried out (TGAQ500, TA Instruments, USA) by heating 10–15 mg of the sample up to 500 °C in a platinum sample cup at the rate of 20 °C/min in the presence of N_2 gas. The samples were analyzed in TGA for degradation of organic matter with increase in temperature. Dried powder sample of nanoparticles was used to carry out XRD, FTIR, and TGA analysis. The pH measurements of reaction solution were performed by using pH meter (Seven Easy pH, METTLER TOLEDO AG, 8603, Switzerland). The hydrodynamic size distribution of the centrifuzed γ-Fe_2O_3 NPs sample was analyzed in a dynamic light scattering (DLS) instrumentation from HORIBA, LB-550 Size Distribution Analyzer. Morphology and selected area electron diffraction (SAED) pattern of as-synthesized γ-Fe_2O_3 NPs were determined using transmission electron microscopy (TEM) by FEI Tecnai, G2 Spirit Twin.

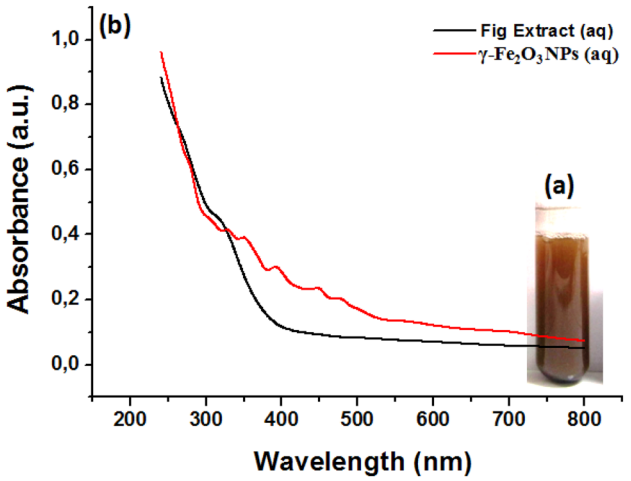

Fig. 1 **a** Photograph of γ-Fe_2O_3 NPs and **b** UV–Vis spectrum of FCF extract and as-synthesized γ-Fe_2O_3NPs

Free radical Scavenging Activity

Antioxidant capacities of FCF coated γ-Fe_2O_3 NPs were determined using DPPH assay as described earlier by Kumar et al. [36] with minor modification. The purified and dried γ-Fe_2O_3 (5 mg) was resuspended in 50 mL water. After that, 1000–200 µL of γ-Fe_2O_3 NPs solution and 1000–1800 µL of H_2O were taken in different test tubes. Then, 2.0 mL of 0.2 mM DPPH fresh solutions (in 95% ethanol) was added and vortexed vigorously. The reaction mixture incubated in the dark for 30 min at room temperature. The absorbance of the reaction mixture was measured spectrophotometrically at 517 nm. The lower absorbance of the reaction mixture indicated a higher percentage of scavenging activity, and the percentage of inhibition of free radicals was determined by the following formula:

$$\text{Scavenging activity}\,(\%) = (A_0 - A_1)/A_0 \times 100 \quad (1)$$

where A_0 is the absorbance of the control (blank, or γ-Fe_2O_3 NPs) and A_1 is the absorbance in the presence of the FeONPs. The final result was expressed as the percentage of DPPH free radical scavenging activity (µg).

Estimation of Total Polyphenolic Content (TPC) in FCFE

The TPC of was estimated by the colorimetric Folin–Ciocalteu's (FC) method, according to Kumar et al. [37]. The 200–800 µL of FCFE, 800–200 µL of H_2O and 2.0 mL of 0.02 N FC reagent were added in a separate glass tube and then mixed well using a Vortex mixer. After that, the reaction mixture was allowed to react for 3 min then 1 mL of 1 N Na_2CO_3 solution was added and mixed well using a Vortex. The solution was incubated in the dark for 120 min at room temperature (23–25 °C). Immediately after completion of reaction, the absorbance was measured at 725 nm using a spectrophotometer and the results were expressed in gallic acid equivalents (GAE; mg/100 g fresh mass) using a gallic acid (0–1 µg/mL) calibration curve. Additional dilution was done if the absorbance value measured was over the linear range of the standard

curve. Each TPC assay was repeated thrice from the same extract in order to determine their reproducibility.

Catalytic activity of γ-Fe_2O_3 NPs

The catalytic efficiency of γ-Fe_2O_3 NPs, was assessed by reduction of 4-NP in the presence of $NaBH_4$ as a model reaction. Briefly, 0.2 mL of 4-NP (2 mM), 20 µg (Set 1) and 100 µg (Set 2) of as-synthesized γ-Fe_2O_3 NPs and 3.6 mL of H_2O were mixed in a 4 mL standard quartz cuvette or (200 µL and 1000 µL of 1 mg/10 mL γ-Fe_2O_3 NPs added in 3.4 and 2.6 mL of H_2O). To this reaction mixture, 0.2 mL of $NaBH_4$ (0.05 mM) solution was added and UV–vis absorption spectra were recorded at different time intervals, leading to a colour change from pale yellow to colourless. Control reactions were also monitored for 30 min in the absence of γ-Fe_2O_3 NPs keeping other parameters constant.The observed rate constant (k) of the reduction process was determined by analyzing the change in an intensity of the peaks at 400 nm as a function of time.The concentration of 4-NP at time t is denoted as C_t, and the initial concentration of 4-NP at t = 0 is regarded as C_0. The C_0/C_t is measured from the relative intensity of absorbance (A_0/A_t).The linear relationship of ln (A_0/A_t) versus time (t) indicates that the reduction of 4-NP by γ-Fe_2O_3 NPs follows the first order kinetics [38].

Results and Discussion

Visual and UV–Vis Spectroscopy

The UV–Vis spectra of diluted FCF extract and as prepared γ-Fe_2O_3 NPs are presented in Fig. 1. The absorption spectra of FCF extract was taken as a baseline and as-synthesized γ-Fe_2O_3 NPs were evaluated. Iron oxide nanoparticles as γ-Fe_2O_3 NPs has been successfully synthesized by using an aqueous extract of *Ficus carica* fruit through green method. During one pot biosynthesis of γ-Fe_2O_3 NPs, a gradual change in greenish-blue colour to brownish-black reaction mixture is observed under vigorous stirring (Fig. 1a) at 75–80 °C, pH 10–11 for 2 h. This clearly indicates the formation of iron oxide nanoparticles/γ-Fe_2O_3 NPs in the reaction mixture. We assume that the FCF extract comprises flavonoids, polyphenolic and coumarins as an antioxidants may be act as primary complexing and reducing agent for the synthesis of γ-Fe_2O_3 NPs [19, 21, 36]. A continuous broad absorption band occurred from 350 to 450 nm ensure the involvement of phytochemicals with Fe^{2+} for the synthesis of γ-Fe_2O_3 NPs. Almost, similar surface plasmon resonance (SPR) spectra of γ-Fe_2O_3 NPs in UV–visible were obtained using the previously reported methods [20, 22].

XRD Analysis

The successful synthesis of γ-Fe_2O_3 NPs and its nature and phase composition with the smallest size were confirmed by XRD analysis. Figure 2 shows the typical XRD pattern

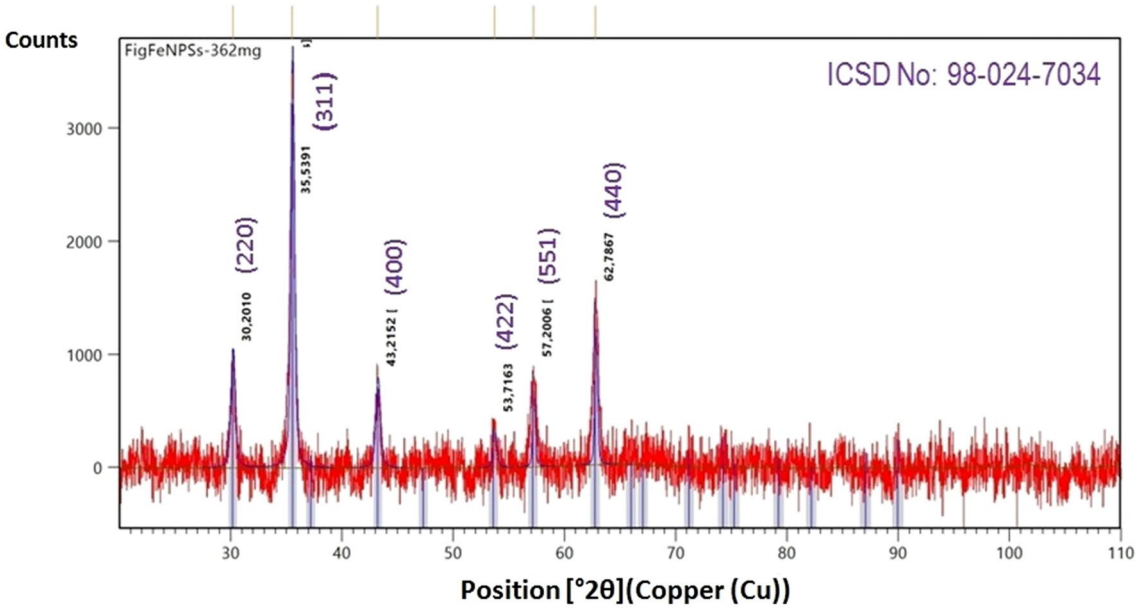

Fig. 2 XRD diffractograms of the iron − FCF extract complex γ-Fe_2O_3 NPs

of as-synthesized single phase γ-Fe_2O_3 (no reflections of impurity) and confirms its high crystalline nature. The XRD peaks, which appeared at 2 theta (2θ) value of 30.20, 35.54, 43.21, 53.72, 57.20 and 62.79° representing (220), (311), (400), (422), (551) and (440) crystallographic planes respectively [39]. The observed Bragg peaks of FCF extract mediated γ-Fe_2O_3 NPs are in agreement with pure phase cubic lattice maghemite γ-Fe_2O_3 with ICSD No: 98-024-7034. It should be noted that the standard XRD patterns of γ-Fe_2O_3 and magnetite (Fe_3O_4) are alike. The characteristic peaks of γ-Fe_2O_3 at 30.20° and 43.21° confirm the formation of γ-Fe_2O_3 NPs and also rules out the fabrication of Fe_3O_4 nanoparticles in sample [40]. Sharp and strong peaks represent a good degree of organization in the particles packing, evidencing the monodispersity (uniform shapes) of the nanoparticles whereas, broad peaks indicate smaller size nanoparticles. The average particle size of the sample was measured by the width of the most prominent XRD peak (311) by using the Debye–Scherrer's equation [21]. The calculated particle size is 3.62 nm and no other peaks relating to other impurities were observed, indicating the single crystalline phase of γ-Fe_2O_3 NPs.

FTIR and TGA Analysis

As a powerful tool, FTIR spectra of the synthesized γ-Fe_2O_3 NPs were recorded by scanning the sample in the range of 400 to 4000 cm^{-1} to analyze the possible biomolecules responsible for the biosynthesis. Figure 3 indicated the surface chemical structure of γ-Fe_2O_3 NPs. The main characteristic peaks of nanoparticles were observed at 441, 477, and 565 cm^{-1} corresponds to Fe–O band vibration (400–700 cm^{-1}), confirming the formation of γ-Fe_2O_3 [39, 41]. The other peaks at 1096, 1355, 1410, 1644, 2793, 2882, 2948 and 3412 cm^{-1} occurred due to the functional groups present in FCF extract. The FTIR band at 1096 cm^{-1} corresponds to C–O–C stretching vibration of alcohol and phenolic groups [21]. The C–O and C–H vibration show a weak band around 1355 and 1410 cm^{-1}. The medium vibrational peak at 1644 cm^{-1} denote the O–H bending and C=O vibration of carbonyl groups [42]. The peaks at 2882 and 2948 cm^{-1} have been attributed to symmetric and unsymmetric C–H stretches in aliphatic compounds [43]. As prepared γ-Fe_2O_3 NPs also exhibit a broad peak near 3412 cm^{-1}, which indicates the presence of hydrogen bonds involved in O–H and adsorbed water molecules [42]. Overall, it is seen that there is a presence of carbonyl, alcohols and phenolic group stuck on the γ-Fe_2O_3 surface even though the FCF extract are washed repeatedly and cannot be removed during the drying process.

The TG analysis of as-synthesized γ-Fe_2O_3 NPs supports the FTIR results. The TGA curve in Fig. 4a indicated a substantial loss in the weight of FCF-γ-Fe_2O_3 NPs between 27 and 500 °C. The decomposition of the FCF organic layer

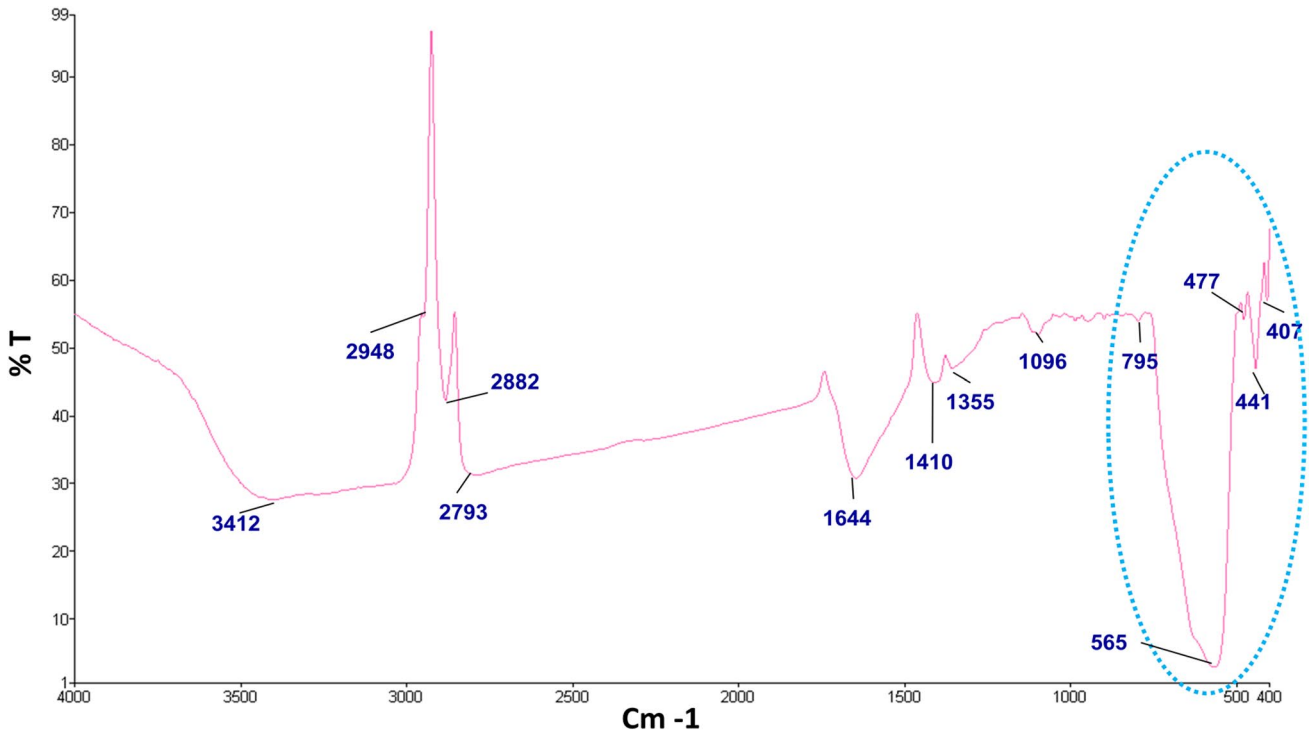

Fig. 3 FTIR spectrum of as-synthesized γ-Fe_2O_3 NPs

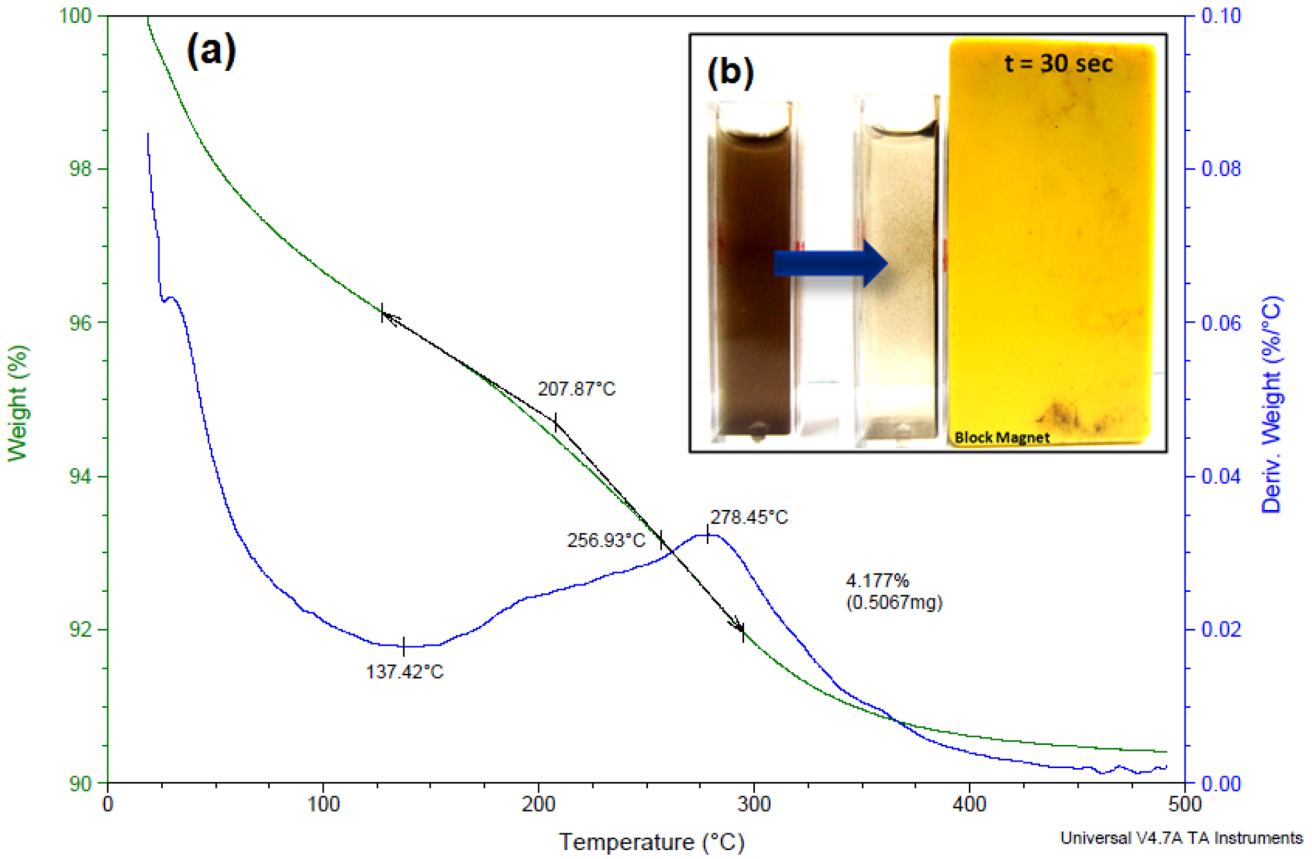

Fig. 4 **a** TG–DTA curve for the FCF extract capped γ-Fe_2O_3 NPs and **b** magnetic separation of as-synthesized γ-Fe_2O_3 NPs using an external magnetic field

was completed at 400 °C. An initial reduction of weight at 27–137.5 °C was observed due to the evaporation of physisorbed/chemisorbed water and other volatile contents present in FCF γ-Fe_2O_3 NPs [44]. A weight loss of 4.18% was noticed from 100 to 300 °C which might be due to the decomposition of biomolecules surrounding the FCF γ-Fe_2O_3 NPs. Additional information was obtained from the first derivative curve analysis that indicated the temperature (T_{max}) at which the degradation rate reached its maximum. The endothermic peak of γ-Fe_2O_3 NPs were found to have a T_{max} of 278.5 °C, which clearly indicates that as prepared γ-Fe_2O_3 NPs contain 92% metal and 4.1% phytochemical coating [20]. From all these results, it is attributable to organic molecule of FCF extract layering on the nanoparticle surface. Figure 4b shows the magnetic separation of as-synthesized γ-Fe_2O_3 NPs using an external magnetic field.

TEM, SAED and DLS Study

Morphology and hydrodynamic diameter of nanoparticles, which were dispersed in water were studied using TEM and DLS. TEM and SAED images of as-synthesized γ-Fe_2O_3 NPs are shown in Fig. 5. According to TEM images (Fig. 5a), fabricated nanoparticles are spherical/dot in shape and size in the range of 4–6 nm. Most of the nanoparticles are embedded in organic matrix, stuck each other and become agglomerated. It is due to interparticle interaction and their size increased in the range of 10 to 50 nm. Figure 5b showed the presence of an organic layer coverage around the γ-Fe_2O_3 NPs and a lower contrast of particles is more embedded in the organic matrix [45]. Figure 5c indicate the SAED analysis. The spotty fring's of micrograph denote the nanocrystalline structure and well pronounced circular diffraction ring confirms the spherical shape of as-prepared γ-Fe_2O_3 NPs [24]. Furthermore, the strong spotty ring has been indexed as (311) and clearly indicate the enhanced crystallinity of the nanoparticles in comparison with the other (hkl) planes in the synthesized γ-Fe_2O_3 NPs, which is evident in the XRD pattern based on their intensity [24]. The DLS method is a measurement based on the Brownian motion of particles and used to determine the size of nanoparticles in colloidal suspension at nanosize scale. In this method, light is sent to the particles and intensity fluctuations in the scattered light are measured [28]. The average particle size of well sonicated and diluted γ-Fe_2O_3 NPs are 6.7 ± 1.7 nm with narrow distribution (Fig. 6). The calculated polydispersity index (PDI) value is 0.064 (< 0.1),

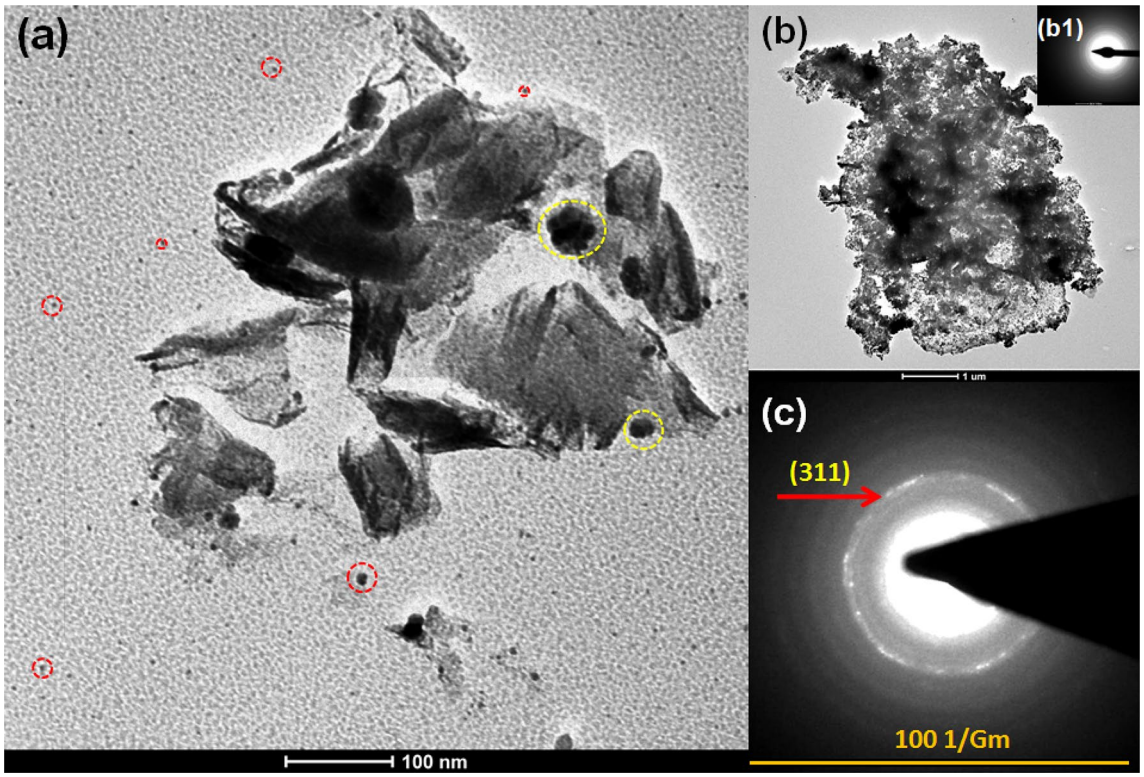

Fig. 5 TEM images (**a**, **b**) and SAED pattern (**c**, **b1**) of biosynthesized γ-Fe_2O_3 NPs

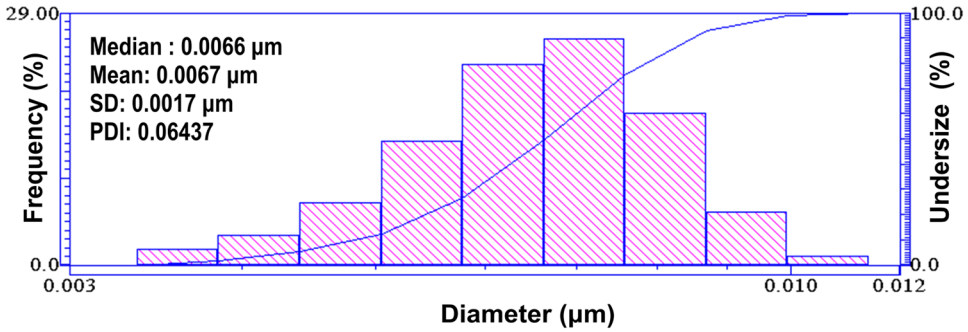

Fig. 6 DLS pattern for ultrasonicated-diluted γ-Fe_2O_3 NPs

therefore its particle distribution will be monodispersive. The size calculated from TEM and DLS gives higher values than those observed by XRD. Finally, all characterization data were well supported the nature and morphology γ-Fe_2O_3 NPs along with the slight difference between the size observed in XRD, TEM and DLS is likely due to the amorphous organic layer and adsorbed species which surround the particles.

Suggested Mechanism for the Biosynthesis of γ-Fe_2O_3 NPs

The FCF extract is rich in high levels of flavonoids, coumarins, chlorogenic acid, organic acids and anthocyanin [29–31]. For the one-pot biosynthesis of γ-Fe_2O_3 NPs via co-precipitation, $Fe(OH)_2$ is starting material and it was prepared by adding 0.1 M NaOH solution to $FeSO_4$

solution and pH is adjusted to 9–10. We believe that $Fe(OH)_2$ oxidized and precipitated as $Fe(OH)_3$ in the presence of oxygen. It was observed that, when FCFE is added to $Fe(OH)_3$ solution, they form an instantaneous brownish-black complex because of the electrostatic interaction between the negatively charged phytochemicals (RO^-, ArO^-, COO^-) and positively charged Fe^{3+} ions. Upon continuous heating at 78–80 °C with continous stirring for 2 h and drying at 90 °C for 12 h, the self-assembled complex of γ-Fe_2O_3 NPs formed.

The possible mechanism for the synthesis of γ-Fe_2O_3 is proposed in Eqs. (2)–(6) [24, 36, 37, 46]:

$$Fe^{2+} + 2H_2O(pH > 9) \rightarrow Fe(OH)_2\downarrow + 2H^+ \quad (2)$$

$$Fe(OH)_2 + [O] \rightarrow Fe(OH)_3\downarrow \quad (3)$$

$$Fe(OH)_3\downarrow + \text{polyphenols/phytochemicals} \rightarrow Fe\text{–phytochemicals complex} \quad (4)$$

$$Fe\text{–phytochemicals complex} + Heat(78\text{–}80\,^{\circ}C) \rightarrow FeO + FeOOH, \alpha - Fe_2O_3NPs\downarrow + Fe_3O_4NPs\downarrow \quad (5)$$

$$Fe_3O_4 + Heat(> 90\,^{\circ}C) \rightarrow \gamma\text{-}Fe_2O_3NPs\downarrow \quad (6)$$

Free Radical Scavenging Activity

Antioxidant applicability of as-synthesized γ-Fe_2O_3 NPs was demonstrated using DPPH as model reagent. Antioxidant activity by as-synthesized γ-Fe_2O_3 NPs is shown in Fig. 7. The result clearly depicted that scavenging activity of the nanoparticles was increased in a dose-dependent manner on DPPH radical with the significant inhibitory rate of 1.18, 2.79, 11.48, 14.54 and 17.01% when the quantity of nanoparticles increases from 20, 40, 60, 80, and 100 µg, respectively. The antioxidant activity of nanoparticles can be attributed to their outer organic layer of nanoparticles, composed of various phyto-constituents of FCF extract which enable them to trap reactive oxygen species (hydroxyl radicals, superoxide anions, singlet oxygen, hydrogen peroxide, etc.) on its spherical surface [36, 37, 47]. This result shows the substantial importance of FCF extract coated-γ-Fe_2O_3NPs as antioxidant and favors the development of various iron oxide-based nanoparticles in therapeutic products.

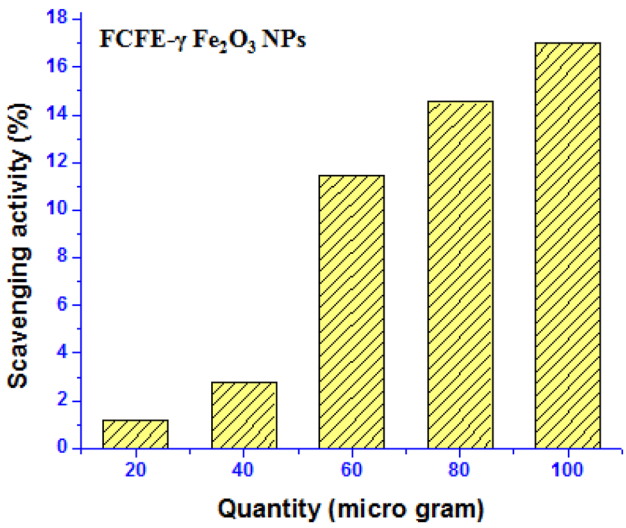

Fig. 7 The DPPH scavenging activity of as-synthesized γ-Fe_2O_3 NPs

Catalytic Activity of γ-Fe_2O_3 NPs

Metal nanoparticles exhibit excellent catalytic properties owing to the high rate of surface adsorption and high surface area to volume ratio [38, 48]. This hypothesis were subjected to testing the catalytic efficacy of γ-Fe_2O_3 NPs, for the reduction of 4-NP to 4-AP as model reaction with $NaBH_4$ at λ_{max} = 400 nm. The kinetics of the reaction were spectrophotometrically studied at 20 µg and 100 µg of biogenic γ-Fe_2O_3NPs and control of the reaction were performed without taking nanoparticle in the reaction mixture, is presented in Fig. 8a. It shows that after the induction time = 30 min, there is a good linear relation between $\ln(A_0/A_t)$ versus time (t) and followed the first-order kinetics. The rates constant were directly calculated from the slope of these plots. The first-order rate constant (k) is highest for FCFE-γ-Fe_2O_3NPs 2 ($k_2 = 49.975 \times 10^{-3}$ min^{-1}, $R^2 = 0.995$) containing 100 µg of γ-Fe_2O_3 NPs whereas, k for FCFE-γ-Fe_2O_3 NPs 1 was decreased more than 6 times with a decreasing quantity of γ-Fe_2O_3 NPs to 20 µg. The observed k_1 and correlation coefficients (R^2) for FCFE-γ-Fe_2O_3NPs 1 were 7.4359×10^{-3} min^{-1} and 0.995. Similarly, $k_{control}$ and R^2 for control reaction were 0.9444×10^{-3} min^{-1} and 0.918. Such diminishing catalytic rates with decrease in nanoparticle quantity can be attributed to a decrease in number of reaction sites, surface area of particles and retards the diffusion of 4-NP to the nanoparticle surface [49]. To understand the mechanism of reduction by 20 and 100 µg of γ-Fe_2O_3 NPs, we plotted UV–vis spectrum from 220–550 nm, shown in Fig. 8 (b, c). Addition of alkali/OH^- to the reaction medium causes deprotonation of 4-NP resulting in the formation of intermediate nitrphenolate ions. The 4-NP shows an absorbance peak at 317 nm, which red shifts to 400 nm due to the formation of 4-nitrophenolate ion. Subsequently added $NaBH_4$ reduces nitrophenolate ion to form 4-AP. In addition of γ-Fe_2O_3 NPs there is a rapid decrease in the intensity of the absorption peak at 400 nm while there

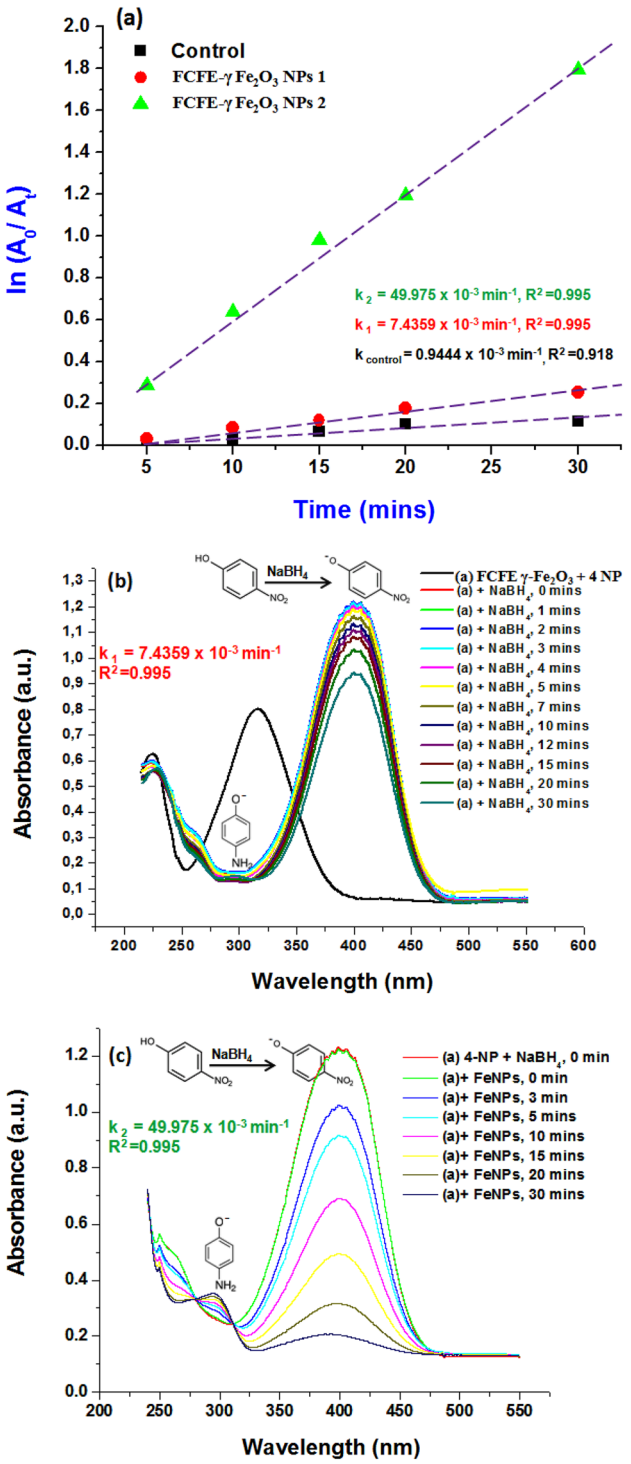

Fig. 8 **a** Plots of $\ln(A_0/A_t)$ for different concentrations of γ-Fe_2O_3 NPs toward the catalytic reduction of 4-NP by $NaBH_4$; **b**, **c** time-dependent UV–Vis spectra of the reduction of 4-NP in the presence of 20 µg and 100 µg γ-Fe_2O_3 nanoparticles

is a concomitant appearance of a new peak at 298 nm (Fig. 8b, c) indicating the formation of reduction product, 4-AP. The decrease in absorbance of 4-NP during the initial minutes of reaction was very slow when the amount of γ-Fe_2O_3NPs were 20 µg but its reaction becomes faster when 100 µg γ-Fe_2O_3NPs was added. Strong nucleophile, BH_4^- acts as electron donor in all reactions. The occurrence of reaction was easily observed with the naked eye owing to the fading of 4-NP yellow colour along with the progress of the reaction [50]. A comparative chart representing the catalytic efficiency of different nanoparticles for the reduction of 4-NP in the presence of $NaBH_4$ as well as present study are summarized in Table 1.

The probable mechanistic pathway for the hydrogenation of 4-NP explained as mention in Fig. 9. Though the reduction of 4-NP to 4-AP using aqueous $NaBH_4$ is thermodynamically favorable (E_0 for 4-NP/ 4-AP = − 0.76 V and H_3BO_3/ BH_4^- = − 1.33 V versus NHE), but the presence of the kinetic barrier due to the large potential difference between donor and acceptor molecules decreases the feasibility of this reaction [51]. To overcome the kinetic energy barrier, BH_4^- ions and 4-nitrophenolate ions co-adsorb on γ-Fe_2O_3 NPs surface. During the catalytic reaction, γ-Fe_2O_3 NPs relay electrons from donor BH_4^- ions by forming Fe–hydride complex, to the acceptor 4-nitrophenolate. Eventually, 4-AP forms and desorbs from the catalyst. The aqueous medium provides the required amount of H^+ ion for complete reduction of 4-NP to 4-AP [52].

Conclusions

In conclusion, we have successfully developed a simple, economical and environment-friendly route to prepare ultrafine γ-Fe_2O_3NPs using an extract of *Ficus carica* fruits. As-prepared γ-Fe_2O_3 NPs were extensively characterized through various spectroscopic and microscopic techniques to interpret its purity, composition, nature and morphology. XRD data showed the presence of pure and single γ-phase of Fe_2O_3 NPs. FTIR results ascertained the specific bands for Fe–O and TGA confirmed the presence of organic coating around the surface of γ-Fe_2O_3 NPs. The resulting nanoparticles are spherical and have average sizes ≈ 4–6 nm confirmed by TEM and DLS. Furthermore, γ-Fe_2O_3NPs showed considerable antioxidant activity against DPPH and catalytic activity for the reduction of 4-Nitrophenol. Such desired

Table 1 A comparative chart representing the catalytic efficiency of different nanoparticles for the reduction of 4-NP in the presence of $NaBH_4$ as well as present study

Nanoparticles	Synthesizing material	Nanoparticle size	Rate constant	Reaction time (min)	Refs.
Silver	*Azadirachta indica* leaf	10–15 nm	0.0794 s^{-1}	30	[48]
Silver	*Breynia rhamnoides* stem	64 nm	4.06×10^{-3} s^{-1}	16	[52]
Gold	*Calothrix* algae	30–120 nm	0.0724752 min^{-1}	16	[53]
Gold	*Breynia rhamnoides* stem	25 nm	9.19×10^{-3} s^{-1}	11	[52]
Gold	Calcium Alginate	< 10 nm	0.14×10^{-5} min^{-1}	45	[54]
Palladium	Xanthan gum	10 nm	0.18309 min^{-1}	24	[55]
Silver/α-Fe_2O_3	Ethylene glycol	140 nm	0.547 min^{-1}	8	[56]
Bentonite clay supported Fe^0 NPs	*Eucalyptus* leaf	10–60 nm	0.1409 min^{-1}	20	[57]
γ-Fe_2O_3	*Ficus carica fruit*	4–6 nm	49.975×10^{-3} min^{-1}	30	This study

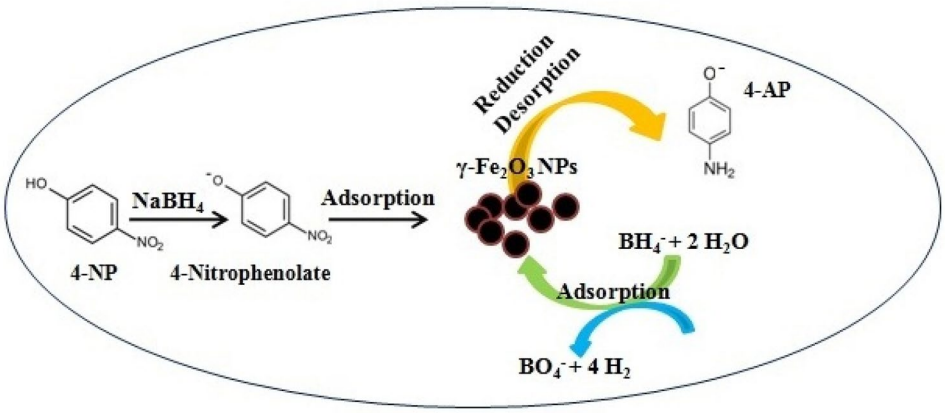

Fig. 9 Suggested mechanism for the γ-Fe_2O_3 NPs mediated catalytic reduction of 4-NP using $NaBH_4$

advantages make these nanoparticles suitable for bioengineering purposes and catalysis.

Acknowledgements This scientific work has been funded by the Universidad de las Fuerzas Armadas ESPE, Ecuador, Prometeo Project of the National Secretariat of Higher Education, Science, Technology and Innovation (SENESCYT), Ecuador and TATA College, India.

Compliance with ethical standards

Conflict of interest The authors confirm they have no conflict of interests.

References

1. Shokrollahi, H.: A review of the magnetic properties, synthesis methods and applications of maghemite. J. Magn. Magn. Mater. **426**, 74–81 (2017)
2. Venkateswarlu, S., SubbaRao, Y., Balaji, T., Prathima, B., Jyothi, N.V.V.: Biogenic synthesis of Fe_3O_4 magnetic nanoparticles using plantain peel extract. Mater. Lett. **100**, 241–244 (2013)
3. Wu, W., He, Q., Jiang, C.: Magnetic iron oxide nanoparticles: synthesis and surface functionalization strategies. Nanoscale Res. Lett. **3**, 397–415 (2008)
4. Laurent, S., Forge, D., Port, M., Roch, A., Robic, C., Vander Elst, L., Muller, R.N.: Magnetic iron oxide nanoparticles: synthesis, stabilization, vectorization, physicochemical characterizations, and biological applications. Chem. Rev. **108**, 2064–2110 (2008)
5. Zhao, M., Josephson, L., Tang, Y., Weissleder, R.: Magnetic sensors for protease assays. Angew. Chem. Int. Ed. **42**, 1375–1378 (2003)
6. Vasantharaj, S., Sathiyavimal, S., Senthilkumar, P., LewisOscar, F., Pugazhendhi, A.: Biosynthesis of iron oxide nanoparticles using leaf extract of *Ruellia tuberosa*: Antimicrobial properties and their applications in photocatalytic degradation. J. Photochem. Photobiol. B **192**, 74–82 (2019)
7. Babay, S., Mhiri, T., Toumi, M.: Synthesis, structural and spectroscopic characterizations of maghemite γ-Fe_2O_3 prepared by one-step coprecipitation route. J. Mol. Struct. **1085**, 286–293 (2015)
8. Seena, S., Kumar, S.: Short-term exposure to low concentrations of copper oxide nanoparticles can negatively impact the ecological performance of a cosmopolitan freshwater fungus. Environ. Sci. Processes Impacts **21**, 2001–2007 (2019)
9. Xu, P., Ming Zeng, G., Huang, D.L., Feng, C.L., Hu, S., Hua Zhao, M., Lai, C., Wei, Z., Huang, C., Xin Xie, G., Feng Liu, Z.: Use of iron oxide nanomaterials in wastewater treatment: a review. Sci. Total Environ. **424**, 1–10 (2012)
10. Banerjee, I., Khollam, Y.B., Balasubramanian, C., et al.: Preparation of γ-Fe_2O_3 nanoparticles using DC thermal arc-plasma route, their characterization and magnetic properties. Scr. Mater. **54**, 1235–1240 (2006)

11. Santra, S., Tapec, R., Theodoropoulou, N., Dobson, J., Hebard, A., Tan, W.: Synthesis and characterization of silica-coated iron oxide nanoparticles in microemulsion: the effect of nonionic surfactants. Langmuir **17**, 2900–2906 (2001)
12. Hasany, S.F., Abdurahman, N.H., Sunarti, A.R., Jose, R.: Magnetic iron oxide nanoparticles: chemical synthesis and applications review. Curr. Nanosci. **9**, 561–575 (2013)
13. Shylesh, S., Schunemann, V., Thiel, W.R.: Magnetically separable nanocatalysts: bridges between homogeneous and heterogeneous catalysis. Angew. Chem. Int. Ed. **49**, 3428–3459 (2010)
14. Martínez-Cabanas, M., López-García, M., Barriada, J.L., Herrero, R., de Vicente, M.E.S.: Green synthesis of iron oxide nanoparticles. Development of magnetic hybrid materials for efficient As (V) removal. Chem. Eng. J. **301**, 83–91 (2016)
15. Groiss, S., Selvaraj, R., Varadavenkatesan, T., Vinayagam Ramesh, R.: Structural characterization, antibacterial and catalytic effect of iron oxide nanoparticles synthesised using the leaf extract of *Cynometra ramiflora*. J. Mol. Struct. **1128**, 572–578 (2017)
16. Al-Ruqeishi, M.S., Mohiuddin, T., Al-Saadi, L.K.: Green synthesis of iron oxide nanorods from deciduous Omani mango tree leaves for heavy oil viscosity treatment. Arab. J. Chem. **12**, 4084–4090 (2019)
17. Kuang, Y., Wang, Q., Chen, Z., Megharaj, M., Naidu, R.: Heterogeneous fenton-like oxidation of monochlorobenzene using green synthesis of iron nanoparticles. J. Colloid Interface Sci. **15**, 67–73 (2013)
18. Huang, L., Weng, X., Chen, Z., Megharaj, M., Naidu, R.: Synthesis of iron-based nanoparticles using oolong tea extract for the degradation of malachite green. Spectrochim. Acta A **117**, 801–804 (2014)
19. Yadav, V.K., Fulekar, M.H.: Biogenic synthesis of maghemite nanoparticles (γ-Fe_2O_3) using *Tridax* leaf extract and its application for removal of fly ash heavy metals (Pb, Cd). Mater. Today Proc. **5**, 20704–20710 (2018)
20. Anchan, S., Pai, S., Sridevi, H., Varadavenkatesan, T., Vinayagam, R., Selvaraj, R.: Biogenic synthesis of ferric oxide nanoparticles using the leaf extract of *Peltophorum pterocarpum* and their catalytic dye degradation potential. Biocatal. Agric. Biotechnol. **20**, 101251 (2019)
21. Ogholbeyg, A.B., Kianvash, A., Hajalilou, A., Abouzari-Lotf, E., Zarebkohan, A.: Cytotoxicity characteristics of green assisted-synthesized superparamagnetic maghemite (γ-Fe_2O_3) nanoparticles. J. Mater. Sci. Mater. Electron. **29**, 12135–12143 (2018)
22. Iqbal, J., Abbasi, B.A., Ahmad, R., Shahbaz, A., Zahra, S.A., Kanwal, S., Munir, A., Rabbani, A., Mahmood, T.: Biogenic synthesis of green and cost effective iron nanoparticles and evaluation of their potential biomedical properties. J. Mol. Struct. **1199**, 126979 (2020)
23. Khalil, A.T., Ovais, M., Ullah, I., Ali, M., Shinwari, Z.K., Maaza, M.: Biosynthesis of iron oxide (Fe_2O_3) nanoparticles via aqueous extracts of *Sageretia thea* (Osbeck) and their pharmacognostic properties. Green Chem. Lett. Rev. **10**, 186–201 (2017)
24. Mohamed, H.E.A., Afridi, S., Khalil, A.T., Ali, M., Zohra, T., Salman, M., Ikram, A.R., Shinwari, Z.K., Maaza, M.: Bio-redox potential of *Hyphaene thebaica* in bio-fabrication of ultrafine maghemite phase iron oxide nanoparticles (Fe_2O_3 NPs) for therapeutic applications. Mater. Sci. Eng. C **112**, 110890 (2020)
25. Demirezen, D.A., Yıldız, Y.S., Yılmaz, S., Yılmaz, D.D.: Green synthesis and characterization of iron oxide nanoparticles using *Ficus carica* (common fig) dried fruit extract. J. Biosci. Bioeng. **127**, 241–245 (2019)
26. Ramirez-Nuñez, A.L., Jimenez-Garcia, L.F., Goya, G.F., Sanz, B., Santoyo-Salazar, J.: *In vitro* magnetic hyperthermia using polyphenol-coated Fe_3O_4@γ-Fe_2O_3 nanoparticles from *Cinnamomun verum* and *Vanilla planifolia*: the concert of green synthesis and therapeutic possibilities. Nanotechnology **29**, 7 (2018). https://doi.org/10.1088/1361-6528/aaa2c1
27. Singh, P.N., Tiwary, D., Sinha, I.: Chromium removal from aqueous media by superparamagnetic starch functionalized maghemite nanoparticles. J. Chem. Sci. **127**, 1967–1976 (2015)
28. Duman, F., Sahin, U., Atabani, A.E.: Harvesting of blooming microalgae using green synthesized magnetic maghemite (γ-Fe_2O_3) nanoparticles for biofuel production. Fuel **256**, 115935 (2019)
29. Lodhil, F., Bradley, M.V., Crane, J.C.: Auxins and gibberellin-like substances in parthenocarpic and non-parthenocarpic syconia of *Ficus carica* L. CV. King. Plant Physiol. **44**, 555–561 (1969)
30. Badgujar, S.B., Patel, V.V., Bandivdekar, A.H., Mahajan, R.T.: Traditional uses, phytochemistry and pharmacology of *Ficus carica*: a review. Pharm. Biol. **52**, 1487–1503 (2014)
31. Duenas, M., Perez-Alonso, J.J., Santos-Buelga, C., Escribano-Bailon, T.: Anthocyanin composition in fig (*Ficus carica* L.). J. Food Comp. Anal. **21**, 107–115 (2008)
32. Du, C., He, S., Gao, X., Chen, W.: Hierarchical Cu@MnO_2 core–shell nanowires: a nonprecious-metal catalyst with an excellent catalytic activity toward the reduction of 4-nitrophenol. ChemCatChem **8**, 2885–2889 (2016)
33. Hava-Ozay, B., Tarımeri, N., Gungor, Z., Demirbakan, B., Ozcan, B., Sezginturk, M.K., Ozay, O.: A new approach to synthesis of highly dispersed gold nanoparticles via glucose oxidase-immobilized hydrogel and usage in the reduction of 4-nitrophenol. ChemistrySelect **5**, 9143–9152 (2020)
34. Zhao, C.Y., Wu, Z., Wang, Y., Yang, C., Li, Y.: Facile fabrication of polystyrene microsphere supported gold-palladium alloy nanoparticles with superior catalytic performance for the reduction of 4-nitrophenol in water. Colloids Surf. A **529**, 417–424 (2017)
35. Kumar, B., Smita, K., Cumbal, L., Debut, A.S.: *Ficus carica* (Fig) fruit mediated green synthesis of silver nanoparticles and its antioxidant activity: a comparison of thermal and ultrasonication approach. BioNanoScience **6**, 15–21 (2016)
36. Kumar, B., Smita, K., Cumbal, L., Debut, A., Galeas, S., Guerrero, V.H.: Phytosynthesis and photocatalytic activity of magnetite (Fe_3O_4) nanoparticles using the Andean blackberry leaf. Mater. Chem. Phys. **179C**, 310–315 (2016)
37. Kumar, B., Smita, K., Galeas, S., Sharma, V., Guerrero, V.H., Debut, A., Cumbal, L.: Characterization and application of biosynthesized iron oxide nanoparticles using *Citrus paradisi* peel: a sustainable approach. Inorg. Chem. Commun. **119**, 108116 (2020)
38. Kumar, B., Smita, K., Cumbal, L., Debut, A.: Phytosynthesis of silver nanoparticles using Andean cabbage: Structural characterization and its application. Mater. Today Proc. **21**, 2079–2086 (2020)
39. Ibrahim-Dar, M., Shivashankar, S.A.: Single crystalline magnetite, maghemite, and hematite nanoparticles with rich coercivity. RSC Adv. **4**, 4105–4113 (2014)
40. Aliahmad, M., Moghaddam, N.N.: Synthesis of maghemite (γ-Fe_2O_3) nanoparticles by thermal-decomposition of magnetite (Fe_3O_4) nanoparticles. Mater. Sci. **31**, 264–268 (2013)
41. Fayazi, M., Ghanei-Motlagh, M., Taher, M.A.: The adsorption of basic dye (Alizarin red S) from aqueous solution on to activated carbon/γ-Fe_2O_3 nano-composite: kinetic and Equilibrium studies. Mater. Sci. Semicond. Process. **40**, 35–43 (2015)
42. Sabbaghan, M., Sofalgar, P.: Single-phase γ-Fe_2O_3 nanoparticles synthesized by green ionothermal method and their magnetic characterization. Ceram. Int. **42**, 16813–16816 (2016)
43. Kumar, S., de Silva, J., Wani, M.Y., Gil, J.M., Sobral, A.J.F.N.: Carbon dioxide capture and conversion by an environmentally friendly chitosan based meso-tetrakis (4-sulfonatophenyl) porphyrin. Carbohydr. Polym. **175**, 575–583 (2017)

44. Ninjbadgar, T., Yamamoto, S.I., Takano, M.: Thermal properties of the γ-Fe_2O_3/poly(methyl methacrylate) core/shell nanoparticles. Solid State Sci. **7**, 33–36 (2005)
45. Magro, M., Campos, R., Baratella, D., Ferreira, M.I., Bonaiuto, E., Corraducci, V., Uliana, M.R., Lima, G.P.P., Santagata, S., Sambo, P., Vianello, F.: Magnetic purification of curcumin from *Curcuma longa* Rhizome by novel naked maghemite nanoparticles. J. Agric. Food Chem. **63**, 912–920 (2015)
46. Gnanaprakash, G., Mahadevan, S., Jayakumar, T., Kalyanasundaram, P., Philip, J., Raj, B.: Effect of initial pH and temperature of iron salt solutions on formation of magnetite nanoparticles. Mater. Chem. Phys. **103**, 168–175 (2007)
47. Harshiny, M., Iswarya, C.N., Matheswaran, M.: Biogenic synthesis of iron nanoparticles using *Amaranthus dubius* leaves extract as reducing agents. Powder Technol. **286**, 744–749 (2015)
48. Singh, J., Kukkar, P., Sammi, H., Rawat, M., Singh, G., Kukkar, D.: Enhanced catalytic reduction of 4-nitrophenol and congo red dye by silver nanoparticles prepared from *Azadirachta indica* leaf extract under direct sunlight exposure. Part. Sci. Technol. **37**, 434–443 (2019)
49. Pradhan, N., Pal, A., Pal, T.: Silver nanoparticle catalyzed reduction of aromatic nitro compounds. Colloids Surf. A **196**, 247–257 (2002)
50. Begum, R., Farooqi, Z.H., Ahmed, E., Naseem, K., Ashraf, S., Sharif, A., Rehan, R.: Catalytic reduction of 4-nitrophenol using silver nanoparticles engineered poly(N-isopropylacrylamide-co-acrylamide) hybrid microgels. Appl. Organomet. Chem. **31**, 1–8 (2016)
51. Singha, J., Mehtab, A., Rawata, M., Basu, S.: Green synthesis of silver nanoparticles using sun dried tulsi leaves and its catalytic application for 4-Nitrophenol reduction. J. Environ. Chem. Eng. **6**, 1468–1474 (2018)
52. Gangula, A., Podila, R., Ramakrishna, M., Karanam, L., Janardhana, C., Rao, A.M.: Catalytic reduction of 4-nitrophenol using biogenic gold and silver nanoparticles derived from *Breynia rhamnoides*. Langmuir **27**, 15268–15274 (2011)
53. Kumar, B., Smita, K., Sánchez, E., Guerra, S., Cumbal, L.: Ecofriendly ultrasound-assisted rapid synthesis of gold nanoparticles using *Calothrix* algae. Adv. Nat. Sci. Nanosci. Nanotechnol. **7**(2), 025013 (2016)
54. Sandip, S., Anjali, P., Subrata, K., Soumen, B.: Tarasankar Pal, Photochemical green synthesis of calcium-alginate-stabilized Ag and Au nanoparticles and their catalytic application to 4-nitrophenol reduction. Langmuir **26**, 2885–2893 (2010)
55. Kumari, A.S., Venkatesham, M., Ayodhya, D., Veerabhadram, G.: Green synthesis, characterization and catalytic activity of palladium nanoparticles by xanthan gum. Appl. Nanosci. **5**, 315–320 (2015)
56. Wang, N., Zeng, S., Yuan, H., Huang, J.: Morphology-dependent interfacial interactions of Fe_2O_3 with Ag nanoparticles for determining the catalytic reduction of p-nitrophenol. J. Environ. Sci. **92**, 1–10 (2020)
57. Sravanthi, K., Ayodhya, D., Swamy, P.Y.: Green synthesis, characterization and catalytic activity of 4-nitrophenol reduction and formation of benzimidazoles using bentonite supported zero valent iron nanoparticles. Mater. Sci. Energy Technol. **2**, 298–307 (2019)